Accelerated Publications

Atomic Force Microscopic Measurement of the Interdomain Angle in Symmetric Holliday Junctions†

Ruojie Sha, Furong Liu, and Nadrian C. Seeman*

Department of Chemistry, New York University, New York, New York 10003

Received January 2, 2002

ABSTRACT: The Holliday junction is a key intermediate in genetic recombination. It consists of four DNA strands that associate by base pairing to produce four double helices flanking a junction point. In the presence of multivalent cations, the four helices, in turn, stack in pairs to form two double-helical domains. The angle between these domains has been shown in a number of solution studies to be ∼60° in junctions flanked by asymmetric sequences. However, the recently determined crystal structure of a symmetric junction [Eichman, B. F., Vargason, J. M., Mooers, B. H. M., and Ho, P. S. (2000) *Proc. Natl. Acad. Sci. U.S.A. 97*, 3971−3976] finds an angle closer to 40°, possibly because of sequence effects. From the crystal structure alone, one cannot exclude the possibility that this unusual angle is a consequence of crystal packing effects. We have formed two-dimensional (2D) periodic arrays of DNA parallelograms with the same junction-flanking sequence used to produce the crystals; these parallelograms are free to adopt their preferred interdomain angle. Atomic force microscopy can be used to establish the interdomain angle in this system. We find that the angle in this junction is 43°, in good agreement with the results of crystallography. We have used hydroxyl radical autofootprinting to establish that the branch point is at the same migratory position seen in the crystals.

The Holliday junction (*1*) is the most prominent DNA intermediate in genetic recombination. It is known to be involved in site specific recombination (*2*−*4*), and it is likely to be involved in homologous recombination (*5*). The Holliday junction consists of four strands of DNA that are paired into four double-helical arms flanking a branch point. This arrangement is shown in the left panel of Figure 1a. The branch point is flanked typically by regions of dyad (homologous) sequence symmetry; this symmetry enables the branch point to relocate through an isomerization known as branch migration (*6*). Much of our information about the physical properties of branched junctions (*7*, *8*) derives from the study of immobile DNA branched junctions (*9*); these are synthetic four-stranded complexes in which the sequence symmetry has been eliminated, thereby fixing the site of the branch point.

In the accepted structural model for the immobile junction in solution, pairs of adjacent arms stack to form two helical domains (*10*). This stacking is derived in the middle and right panels of Figure 1a, where the double-helical arms of the Holliday junction are emphasized, rather than its strands. The favored stacking structure is a function of the base pairs in the vicinity of the junction (*11*). The right-most panel shows how the angles between two helical arms collapse to form the two-domain stacking structure shown in the left panel of Figure 1b. This structure leads to a molecule in which two "helical" strands have a structure similar to strands in conventional DNA double helices, and the other two "crossover" strands connect the domains. This arrangement is evident in the left panel of Figure 1b. The helical domains are oriented about 60° from antiparallel (a 60° right-handed twist) to each other; this feature has been established in solution by fluorescence resonance energy transfer (FRET)[1] (*12*), and by time-resolved FRET (*13*), and confirmed recently by atomic force microscopy (AFM) (*14*). This 60° angle is illustrated in the right panel of Figure 1b, where the structure in the left panel has been rotated 90° about the horizontal axis.

Recently, Ho and his colleagues have determined the crystal structure of a symmetric junction (*15*). This structure confirms the key features of this model, but finds an angle

† This research has been supported by Grants GM-29554 from the National Institute of General Medical Sciences, N00014-98-1-0093 from the Office of Naval Research, CTS-9986512, EIA-0086015, DMR-01138790, and CTS-0103002 from the National Science Foundation, and F30602-01-2-0561 from DARPA/AFOSR.

* To whom correspondence should be addressed. E-mail: ned.seeman@nyu.edu.

[1] Abbreviations: 2D, two-dimensional; 3D, three-dimensional; AFM, atomic force microscopy; DS, double-stranded DNA; EDTA, ethylenediaminetetraacetic acid; FRET, fluorescence resonance energy transfer; HEPES, *N*-(2-hydroxyethyl)piperazine-*N*′-2-ethanesulfonic acid; HJ, Holliday junction; TAEMg, solution containing 40 mM Tris-HCl (pH 8.0), 20 mM acetic acid, 2 mM EDTA, and 12.5 mM magnesium acetate; dApdC, dinucleoside phosphate whose 5′ nucleoside is adenosine and whose 3′ nucleoside is cytidine; dGpdT, dinucleoside phosphate whose 5′ nucleoside is guanosine and whose 3′ nucleoside is thymidine.

10.1021/bi020001z CCC: $22.00
Published on Web 04/20/2002

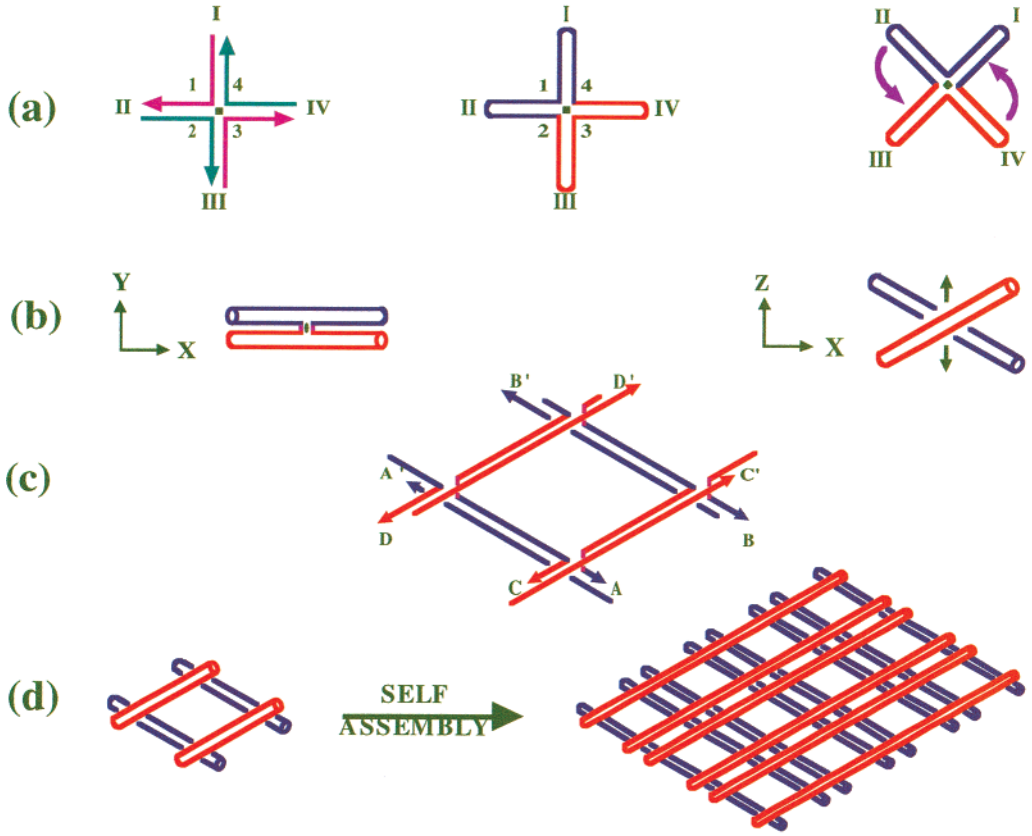

FIGURE 1: Schematic representations of the Holliday junction, its use as a parallelogram component, and their assembly into 2D arrays. (a) Representations of the Holliday junction. The left panel shows the Holliday junction as four strands, in two homologous pairs, as represented by the colors. The middle panel represents the same structure, but emphasizing its helical structure; here, adjacent helices are colored the same. The right panel rotates the molecule and indicates with curved arrows the folding of the helices into a stacked structure. (b) Stacked structure. The left panel shows a view down the dyad axis of the Holliday junction. The dyad axis is denoted by the small lens-shaped figure. The upper helical domain is rotated 30° about the vertical axis so that its right end penetrates the page, and the lower helical domain is rotated 30° about the vertical axis so that its left end penetrates the page. The *X* and *Y* axes of a right-handed coordinate system are shown to help orient the reader. The right panel shows a view with the dyad axis vertical. The molecule has been rotated 90° about the *X* axis. The dyad axis is represented by the double arrows. (c) Strand structure of the rhombus-like motif. The strand structure of the molecule is shown. Arrowheads denote 3′ ends of strands. Sticky ends are shown by the letters A−D, and A′−D′ represent their respective complements. The molecule is constructed from the strands synthesized as shown, rather than from the ligation of four junctions. The ultimate parallel helices are drawn in identical colors (red and blue). (d) Schematic representation of the parallelogram and its self-assembly into a 2D array. In the left panel, four molecules, in the orientation of the right part of panel b, are combined. There are six turns of DNA in each helix, and four turns between crossover points, leading to one-turn overhangs on the ends. The red helices are ~2 nm closer to the reader than the blue helices. The right panel shows the 2D self-assembly product of the motif; the long separations between helices contain four helical turns, and the short separations contain two helical turns. Note that the latticework array contains two separate layers, an upper layer oriented from the lower left to the upper right and a lower layer oriented from the lower right to the upper left.

of ~40° between the domains. The authors of that work ascribe the unusual angle to sequence-dependent interdomain hydrogen bonding. However, from the crystal structure alone, it is not possible to exclude the possibility that the angle is a consequence of crystal packing forces. An independent measurement of the angle by a different technique is required for that exclusion, and we have done that here, using AFM.

We have reported a system for measuring the interdomain angle of Holliday junctions by AFM observation of two-dimensional periodic arrays of Holliday junction parallelograms (*14*). The strand structure of a DNA parallelogram is shown in Figure 1c, and a schematic of the parallelogram is shown in the left panel of Figure 1d. The drawing of the parallelogram in Figure 1d also shows that these parallelograms are actually 3D figures, with the red pair of parallel edges (helices) ~2 nm closer to the reader than the blue pair. The self-assembly of these parallelograms into two-dimensional arrays is illustrated schematically on the right of Figure 1d. Examination of these arrays using atomic force microscopy (AFM) permits one to measure both the sign and the magnitude of the interdomain angle. This information is readily available from the autocorrelation function of the AFM image. We have used this method to characterize both antiparallel immobile conventional junctions (*14*) and parallel bowtie junctions, which contain 5′,5′ and 3′,3′ linkages in their crossover strands (*16*). A key feature of this system is that the junctions are free to relax to the most favorable angle. We have shown that the measurements are independent of substrate (*16*), and are capable of reporting the angle to an error of a few degrees. Here, we have used this method to measure the angle between helical domains in a junction whose crossover-flanking sequences are the same as those in the molecule studied by Ho and his colleagues. We find that the angle measured is indeed very close to that seen in the crystal structure, and we thereby exclude crystal packing forces as the key contributor to the interdomain angle in this junction.

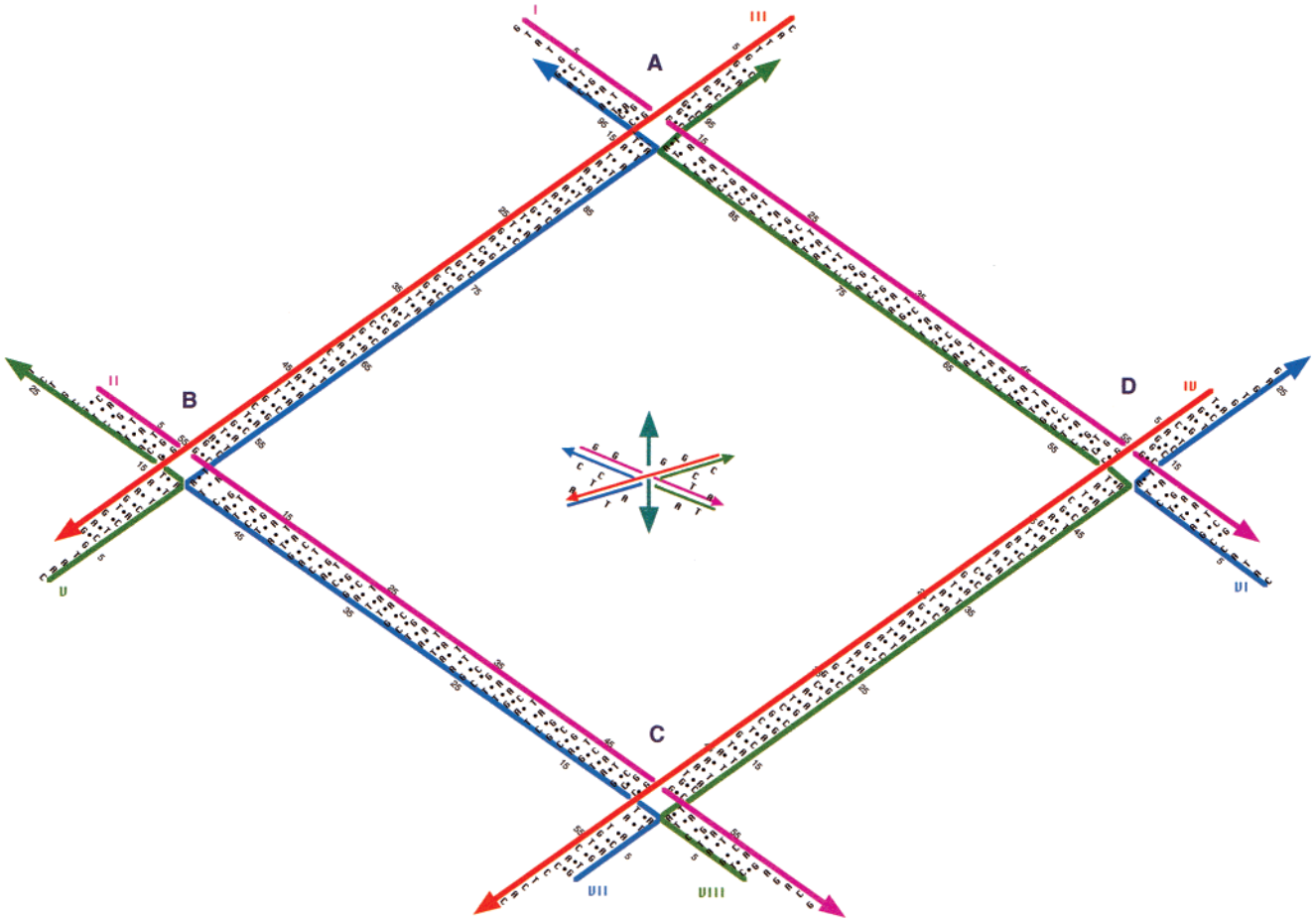

FIGURE 2: Sequence of the parallelogram. The individual junctions are labeled A−D, and nucleotide numbering is shown to correlate with Figure 4. Arrowheads denote the 3′ ends of the strands. The approximate structure of the junction is indicated. The drawing in the center indicates the sequence of the junction used at each vertex, showing that the crossover strands all have the sequence TACC, as used in the crystal structure. The vertical double-headed arrow denotes the axis of dyad symmetry.

MATERIALS AND METHODS

DNA Design, Synthesis, and Purification. All DNA molecules used in this study were designed using the program SEQUIN (*17*). The sequences and strand numbering are shown in Figure 2. The strands were synthesized on an Applied Biosystems 380B automatic DNA synthesizer, removed from the support, and deprotected using routine phosphoramidite procedures (*18*). DNA strands have been purified by denaturing gel electrophoresis; bands were cut out of 12 to 20% denaturing gels and eluted in a solution containing 500 mM ammonium acetate, 10 mM magnesium acetate, and 1 mM EDTA.

Formation of Hydrogen-Bonded Complexes and Arrays. Parallelogram complexes were formed by mixing a stoichiometric quantity of each strand (50 nM), as estimated by OD_{260}, in 5 mM HEPES (pH 7.0), 2 mM $MgCl_2$, and 0.5 mM EDTA. This mixture was cooled slowly from 90 °C to room temperature in a 1 L water bath to produce individual parallelograms. The two-dimensional arrays contained only a single parallelogram, so this protocol was sufficient for their production.

AFM Imaging. A 3−5 μL sample drop was spotted on freshly cleaved mica (Ted Pella, Inc.) and left to adsorb to the surface for 2 min. To remove buffer salts, 5−10 drops of doubly distilled water was placed on the mica, the drop was shaken off, and the sample was dried with compressed air. Imaging was performed in contact mode under 2-propanol in a fluid cell on a NanoScope II instrument, using commercial 200 μm cantilevers with Si_3N_4 tips (Digital Instruments). The feedback setpoint was adjusted frequently to minimize the contact force to be approximately 1−5 nN.

Hydroxyl Radical Analysis. Individual strands of the complexes are radioactively labeled, and are additionally gel purified from a 15% denaturing polyacrylamide gel. Each of the labeled strands (approximately 10 pmol in TAEMg) is annealed to a 4-fold excess of the unlabeled complementary strand, annealed to the complex, as described above, left untreated as a control, or treated with sequencing reagents (*19*) for a sizing ladder. The samples are annealed as described above. Hydroxyl radical cleavage of the double-strand and junction samples for all strands takes place for 2 min (*20*), with modifications noted by Churchill et al. (*10*). The reaction is stopped by addition of thiourea, and the mixture is then precipitated with ethanol. The sample is dried, dissolved in a formamide/dye mixture, and loaded directly onto a 14% polyacrylamide/8.3 M urea sequencing gel. Autoradiograms are analyzed on a BioRad GS-525 molecular imager.

Polyacrylamide Gel Electrophoresis. Conventional denaturing gels, sequencing denaturing gels, and nondenaturing gels have been prepared and run as described previously (*21*).

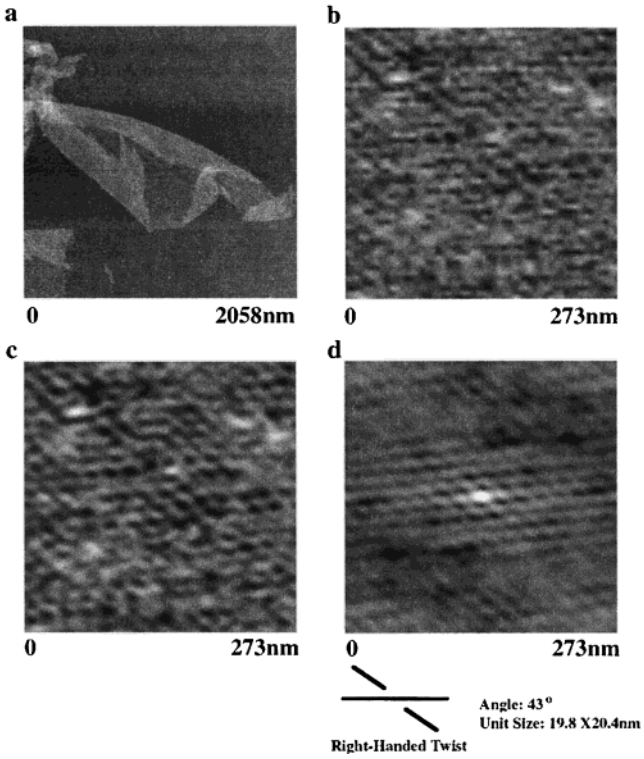

FIGURE 3: Atomic force microscopy of a parallelogram array. The image in the upper left is an unzoomed view of a 2D array formed by the parallelogram containing the sequence used for the crystal structure (*15*). The panel in the upper right is a zoom of this image, and the panel in the lower left contains a Fourier-smoothed image of the zoomed image. The panel in the lower right is the autocorrelation function of the smoothed image. An interpretation of the image is shown at the bottom of this panel, indicating that the angle between the helical directions is ~43°, and also showing the periodicities in the two directions.

RESULTS

Two-Dimensional Arrays of Symmetric Holliday Junctions. Figure 1d illustrates that a parallelogram can form an array with two different spacings, one corresponding to the area enclosed within the parallelogram and the other corresponding to the interparallelogram spacing. In the experiments we have performed, the vertices of the parallelogram are separated by four turns of DNA (42 nucleotide pairs), and the interparallelogram spacing is two turns of DNA. Thus, the periodicity of the array is expected to be ~63 nucleotide pairs in each direction, corresponding to ~21.4 nm. The sequence of the parallelogram molecule that was used is shown in Figure 2. Each junction is flanked by the same dinucleotide sequences (GG·CC and TA·TA) that flank the junction symmetrically in the structure reported by Ho and his colleagues (*15*).

AFM Visualization of Two-Dimensional Arrays. Figure 3 illustrates the results of the AFM experiments. Figure 3a shows a distant view of one of the parallelogram arrays. Its dimensions are roughly 2 μm × 1 μm, but the outer portions of the array are folded over it. Nevertheless, a well-defined lattice is evident in the section that is exposed directly to view. The resolution of the image does not afford a clear resolution of the two closest helices in the image, but fuses them into a single linear feature. Figure 3b is a zoomed picture of this array that focuses on the features of the array. There is a lot of noise in this image, but it is clear that there is a prominent horizontal component to the image. A second component is also visible along a roughly upper-left to lower-right diagonal.

Fourier smoothing of the image (Figure 3c) reveals features more clearly. A rhomboid-shaped array of bumps is clear in this image. Mao et al. (*14*) showed that these bumps are produced by the smallest parallelograms (two turns × two turns) in the structure, where the top helices (red in Figure 1d) of the small rhombus are not flexible enough to make contact with the mica layer below. Counting bumps along the nearly horizontal direction reveals ~13 intervals in the 273 nm wide field, an average of 21 nm per interval, in good agreement with the expected periodicity. The autocorrelation function of this image, shown in Figure 3d, gives a clear image of the repetitive features of the array. It is clear that the horizontal direction is above the diagonal direction in this view. The periodicity is readily measured to be 19.8 nm × 20.4 nm. Most importantly, the angle between the two directions is also clear in this image. It is seen to be 43°, in excellent agreement with the value determined by crystallography. The observed angle is independent of whether the scanning is done in the up or down direction. It is also independent of the orientation of the crystalline array.

Hydroxyl Radical Autofootprinting of Junctions in Parallelograms. The parallelograms contain partially mobile junctions wherein the branch point can, in principle, occupy five different loci through branch migration. It is necessary to show that the array is in the same migratory position seen in the crystal structure before the sequence dependence of the structure can be ascertained. We have used hydroxyl radical autofootprinting previously to establish the position of the branch point in both fixed (*10*, *22*) and symmetric (*21*, *23*, *24*) immobile molecules. These experiments are performed by labeling a component strand of the complex and exposing it to hydroxyl radicals. The key feature noted in these analyses is decreased susceptibility to attack when comparing the pattern of the strand as part of the complex, relative to the pattern derived from linear duplex DNA. Decreased susceptibility is interpreted to suggest that access to the hydroxyl radical may be limited by steric factors at the sites where it is detected. Likewise, similarity to the duplex pattern at points of potential flexure is assumed to indicate that the strand has adopted a helical structure in the complex, whether it is required by the secondary structure.

The hydroxyl radical autofootprints of the four junctions in the parallelogram are shown in Figure 4. The pattern of each of the four strands of each junction is shown, as both the sequence in the parallelogram and the same sequence as duplex DNA. In each case, the strands designed to be the crossover strands are in the first and third panels. The positions of the junction sites seen in the crystal structure are denoted by vertical arrows. In each case, the greatest relative protection is at the sites denoted by the arrows, indicating that the junctions are at the expected sites. Thus, the sequences that flank the junction in the crystal structure also flank the junction in the parallelograms.

DISCUSSION

Measurement of the Angle between Helical Domains. We have used analysis of the parallelogram array autocorrelation function to measure the angle between the helical domains

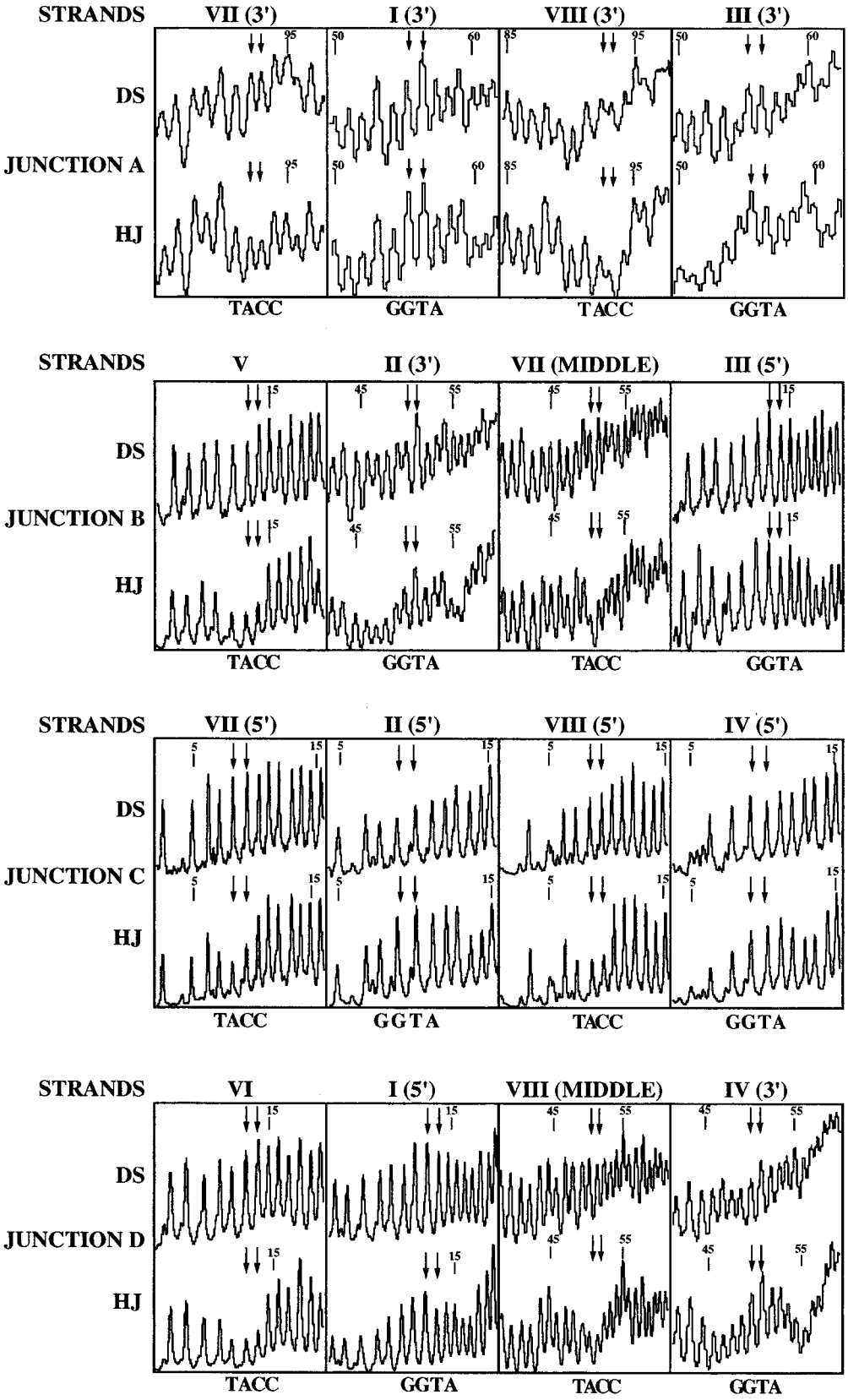

FIGURE 4: Hydroxyl radical protection profiles of the four junctions. Each junction is displayed and labeled A, B, C, or D. The patterns are densitometric scans of sequencing gels used to analyze the protection patterns. Two patterns are shown for each junction, one for the pattern produced by the strand in linear duplex DNA (DS) and one for it in the Holliday junction that is part of the parallelogram (HJ). The strands correspond to the labeling in Figure 2. The crossover strands are in the first and third panels, and the helical strands are in the second and fourth panels in all cases. Nucleotide positions are denoted by numbers. The position on the numbered strand is indicated above each panel. The expected junction positions, corresponding to the position in the crystal structure, are denoted by downward-pointing arrows. The junction-flanking nucleotides are drawn under each panel. Note the extensive protection in the HJ strand at the expected positions.

of a symmetric Holliday junction. The value that we obtain is in very good agreement with the angle seen in the crystal structure (*15*). This value is markedly different from the angles determined previously in immobile systems, both in solution (*12*, *13*) and in the same analytical system used here (*14*). Crystal structures of related systems (*25*, *26*) also report different interdomain angles. Thus, we have used an independent method to establish the angle between helical domains. The agreement between the two methods of measurement validates the results obtained by both. It is clear that the interdomain angle observed by Ho et al. (*15*) is not a consequence of crystal packing.

Measurement of Junction Thermodynamic Quantities. We have demonstrated that the branch point is located at the position found in the crystal structure. This finding suggests that the hydrogen bonding found in the crystal structure indeed provides stabilization that maintains the structure. We have reported earlier (*27*) the thermodynamics of symmetric sequences that may flank Holliday junctions. We found that the same dApdC sequence (dGpdT in the notation of ref *27*) was one of the most favored sequences. However, it is unclear whether the hydrogen bonding thought to stabilize the structure could have contributed significantly to those measurements, because the helices were held strictly antiparallel in that system. The development of a new parallelogram-based type of symmetric immobile junction (C. Mao, S. Liao, and N. C. Seeman, in preparation) that preserves the interdomain angle is expected to facilitate the determination of more accurate values for the thermodynamic quantities that characterize the behavior of the symmetric Holliday junction.

REFERENCES

1. Holliday, R. (1964) *Genet. Res. 5*, 282−304.
2. Hoess, R., Wierzbicki, A., and Abremski, K. (1987) *Proc. Natl. Acad. Sci. U.S.A. 84*, 6840−6844.
3. Kitts, P. A., and Nash, H. A. (1987) *Nature 329*, 346−348.
4. Nunes-Duby, S. E., Matsumoto, L., and Landy, A. (1987) *Cell 50*, 779−788.
5. DasGupta, C., Wu, A. M., Kahn, R., Cunningham, R. P., and Radding, C. M. (1981) *Cell 25*, 507−516.
6. Hsieh, P., and Panyutin, I. G. (1995) *Nucleic Acids Mol. Biol. 9*, 42−65.
7. Lilley, D. M. J., and Clegg, R. M. (1993) *Annu. Rev. Biophys. Biomol. Struct. 22*, 299−328.
8. Seeman, N. C., and Kallenbach, N. R. (1994) *Annu. Rev. Biophys. Biomol. Struct. 23*, 53−86.
9. Seeman, N. C. (1982) *J. Theor. Biol. 99*, 237−247.
10. Churchill, M. E. A., Tullius, T. D., Kallenbach, N. R., and Seeman, N. C. (1988) *Proc. Natl. Acad. Sci. U.S.A. 85*, 4653−4656.
11. Chen, J.-H., Churchill, M. E. A., Tullius, T. D., Kallenbach, N. R., and Seeman, N. C. (1988) *Biochemistry 27*, 6032−6038.
12. Murchie, A. I. H., Clegg, R. M., von Kitzing, E., Duckett, D. R., Diekmann, S., and Lilley, D. M. J. (1989) *Nature 341*, 763−766.
13. Eis, P., and Millar, D. P. (1993) *Biochemistry 32*, 13852−13860.
14. Mao, C., Sun, W., and Seeman, N. C. (1999) *J. Am. Chem. Soc. 121*, 5437−5443.
15. Eichman, B. F., Vargason, J. M., Mooers, B. H. M., and Ho, P. S. (2000) *Proc. Natl. Acad. Sci. U.S.A. 97*, 3971−3976.
16. Sha, R., Liu, F., Millar, D. P., and Seeman, N. C. (2000) *Chem. Biol. 7*, 743−751.
17. Seeman, N. C. (1990) *J. Biomol. Struct. Dyn. 8*, 573−581.
18. Caruthers, M. H. (1985) *Science 230*, 281−285.
19. Maxam, A. M., and Gilbert, W. (1980) *Methods Enzymol. 65*, 499−560.
20. Tullius, T. D., and Dombroski, B. A. (1985) *Science 230*, 679−681.
21. Sha, R., Liu, F., and Seeman, N. C. (2000) *Biochemistry 39*, 11514−11522.
22. Li, X., Wang, H., and Seeman, N. C. (1997) *Biochemistry 36*, 4240−4247.
23. Zhang, S., Fu, T.-J., and Seeman, N. C. (1993) *Biochemistry 32*, 8062−8067.
24. Zhang, S., and Seeman, N. C. (1994) *J. Mol. Biol. 238*, 658−668.
25. Ortiz-Lombardia, M., Gonzalez, A., Eritja, R., Aymami, J., Azorin, F., and Coll, M. (1999) *Nat. Struct. Biol. 6*, 913−917.
26. Nowakowski, J., Shim, P. J., Prasad, G. S., Stout, C. D., and Joyce, G. F. (1999) *Nat. Struct. Biol. 6*, 151−156.
27. Sun, W., Mao, C., Liu, F., and Seeman, N. C. (1998) Sequence Dependence of Branch Migratory Minima, *J. Mol. Biol. 282*, 59−70.

BI020001Z